

Supporting information

Enhancing hydrogen evolution activity by doping and tuning the curvature of manganese-embedded carbon nanotubes

Haijun Liu, Lianming Zhao,* Yonghui Liu, Houyu Zhu, Jing Xu, and Wenyue Guo*

School of Materials Science and Engineering, Institute of Advanced Materials, China

University of Petroleum, Qingdao, Shandong 266580, People's Republic of China.

E-mail: lmzhao@upc.edu.cn (L. Zhao).

wyguo@upc.edu.cn (W. Guo).

Table of contents

1. Structural parameters of pristimne CNTs.....	S-4
2. Structural parameters, and Mn binding energy for MnCNTs and MnN ₂ CNT(5,5)	
.....	S-5
3. Adsorption energies for FHA and SHA on MnCNTs and MnN ₂ CNT(5,5)	S-6
4. Structural parameters and Hirshedl charges for FHA and SHA on MnCNTs and	
MnN ₂ CNT(5,5)	S-7
5. Bond angle sum around the active ortho-C site for MCNTs (M = Mn and Co) ..	S-8
6. Monatomic substitution at a monocacancy and divacancy of CNT(5,5).....	S-9
7. Representative configurations and definition of important structural parameters for	
CNTs, MnCNTs, and MnN ₂ CNT(5,5)	S-
10	
8. The electron deficiency center of di-vacant CNTs and N ₂ CNT(5,5)	S-
11	
9. The detailed projected density of states of MnCNT(5,5) and CoCNT(5,5)	S-12
10. The energy band structures of MnCNTs	S-13
11. The PDOS of pristine and first hydrogen adsorbed MnCNTs and	
MnN ₂ CNT(5,5).....	S-14
12. The final structures of MnCNT(5,5) after 1 ps first-principle molecular dynamics	
simulations	S-15
13. The change of Mn–C bond length in MnCNT(5,5) in first-principle molecular	
dynamics simulation	S-16
14. The phonon dispersion spectrum of MnCNT(5,5)S-17
15. All possile adsorption sites for first and second hydrogen on MnCNTs and	
MnN ₂ CNT(5,5)	S-18
16. The stable configurations of FHA and SHA on MnCNTs and MnN ₂ CNT(5,5)	
.....	S-20
17. The radial distribution of H atoms for MCNT(5,5) and MN ₂ CNT(5,5) (M = Mn	
and Co)	S-21

18. The relationship between activation barrier and absolute hydrogen adsorption energy on MnCNTs and MnN ₂ CNT(5,5).....	S-
22	
19. The electronic potential profiles of MnCNT(5,5) and CoCNT(5,5)	S-23
20. The possible configurations of MnN ₂ CNT(5,5)	S-24

Table S1. The calculated bond lengths d (in Å) and bond angles θ (in °) of pristine CNTs.^a

Species	CNT(3,3)	CNT(4,4)	CNT(5,5)	CNT(6,6)	CNT(7,7)	CNT(9,9)
d_1	1.440	1.431	1.429	1.428	1.427	1.426
			1.427, ¹ 1.422, ² 1.429 ³		1.423 ²	1.425 ²
d_2/d_3	1.431	1.427	1.418	1.424	1.418	1.417
			1.423, ¹ 1.426 ²		1.422 ¹	1.422 ¹
θ_1	118.48	118.97	118.63	119.38	118.94	119.06
θ_2/θ_3	116.29	117.99	119.05	119.19	119.68	119.96

^aThe structural parameters are defined in Figure S2.

1. G. Y. Sun, J. Kurti, M. Kertesz and R. H. Baughman, *J. Phys. Chem. B*, 2003, 107, 6924–6931.
2. Z. Zhou, M. Steigerwald, M. Hybertsen, L. Brus and R. A. Friesner, *J. Am. Chem. Soc.*, 2004, 126, 3597–3607.
3. L. H. Gan and J. Q. Zhao, *Phys. E*, 2009, 41, 1249–1252.

Table S2. Calculated bond lengths d (in Å),^a bond angles θ (in °),^a Mn binding energies E_b (in eV), and energy difference (ΔE_b) (in eV) between E_b and the cohesive energy E_{coh} for Mn embedded and Mn and N co-embedded CNTs.^b

Species	MnCNT(3,3)	MnCNT(4,4)	MnCNT(5,5)	MnCNT(6,6)	MnCNT(7,7)	MnCNT(9,9)	MnN ₂ CNT(5,5)
Δd_{Mn}^c	0.810	0.753	0.751	0.722	0.720	0.694	0.666
d_1	1.411	1.411	1.411	1.409	1.410	1.412	1.409
d_2	1.905	1.910	1.906	1.905	1.913	1.919	1.899
d_3	1.420	1.415	1.406	1.408	1.404	1.402	1.407
d_4	1.449	1.441	1.439	1.433	1.434	1.432	1.434
d_5	1.417	1.414	1.409	1.413	1.409	1.409	1.411
d_6							1.366
d_7							1.915
d_8							1.366
θ_1	109.23	104.36	102.99	102.29	102.88	102.88	102.48
θ_2	116.41	116.80	117.32	117.49	117.46	117.51	117.65
θ_3	132.33	135.83	138.63	139.85	139.57	139.60	138.34
θ_4	121.59	122.22	121.97	122.07	122.43	122.66	121.630
θ_5	109.29	111.02	112.38	113.44	113.57	114.33	114.26
θ_6	117.20	118.66	119.51	119.95	120.14	120.32	118.37
E_b	-7.62	-7.61	-7.02	-6.37	-6.21	-5.33	-5.85
ΔE_b	-3.89	-3.88	-3.29	-2.64	-2.48	-1.60	-2.12

^a The structural parameters are defined in Figure S2.

^b The notations of the energies are defined in the section of method and computational method.

^c Δd_{Mn} is the distance between the Mn atom and the plane formed by four *ortho*-C atoms.

Table S3. Calculated adsorption energies E_{ads} (in eV) for first (FHA) and second (SHA) hydrogen atoms adsorbed on possible adsorption sites of Mn embedded and Mn and N co-embedded CNTs.^{a,b}

Adsorption site		MnCNT(3,3)	MnCNT(4,4)	MnCNT(5,5)	MnCNT(6,6)	MnCNT(7,7)	MnCNT(9,9)	MnN ₂ CNT(5,5)
FHA	T1	0.23	0.19	0.14	0.13	0.13	0.11	0.01
	T3/T4	-0.37	-0.24	-0.15	-0.12	-0.10	-0.09	-0.22/0.60
	T5/T10	-0.26	0.13	0.34	0.47	0.52	0.60	0.23/0.52
	T6/T9	-0.09	0.37	0.58	0.69	0.79	0.90	0.56/0.21
	T7/T8	-0.36	0.04	0.31	0.44	0.54	0.68	0.30/-0.19
SHA	T1	0.04	0.01	-0.09	-0.12	-0.12	-0.18	-0.04
	T2	-0.30	-0.03	0.18	0.28	0.32	0.38	0.09
	T4	-0.46	-0.41	-0.39	-0.36	-0.23	-0.18	0.49
	T6	-0.39	0.05	0.26	0.31	0.43	0.49	0.17
	T7	-0.91	-0.65	-0.48	-0.46	-0.29	-0.20	-0.33

^a The adsorption sites are defined in Figure S10.

^b The T3 site is occupied by first hydrogen atom in consideration of the adsorption sites for second hydrogen atoms.

Table S4. Calculated bond lengths d (in Å),^a bond angles θ (in °),^a and Hirshfeld charges q (in e) for first (FHA) and second (SHA) hydrogen atom adsorbed on Mn embedded and Mn and N co-embedded CNTs.

Species	MnCNT(3,3)	MnCNT(4,4)	MnCNT(5,5)	MnCNT(6,6)	MnCNT(7,7)	MnCNT(9,9)	MnN ₂ CNT(5,5)	
FHA	$d_{\text{C-H}}$	1.114	1.131	1.140	1.142	1.148	1.150	1.144
	d_2	2.045	2.002	1.989	2.031	1.994	2.001	1.984
	d_3	1.484	1.470	1.437	1.457	1.451	1.449	1.458
	θ_1	101.29	104.28	103.99	105.45	104.63	105.20	104.27
	θ_2	108.11	111.94	113.43	113.23	114.50	114.90	112.45
	θ_3	120.41	128.08	131.65	131.71	133.81	134.34	130.6
	θ_4	120.36	121.19	120.87	121.28	121.14	121.28	120.9
	θ_5	114.67	113.75	114.49	114.86	115.35	115.88	116.25
	θ_6	116.65	118.75	119.62	120.05	120.32	120.58	119.04
	q_{Mn}	0.217	0.201	0.193	0.189	0.187	0.183	0.196
SHA	$q_{\text{ortho-C}}$	-0.085	-0.075	-0.068	-0.065	-0.064	-0.062	-0.065
	q_{H}	0.043	0.047	0.046	0.045	0.043	0.042	0.041
	$d_{\text{C-H}}$	1.109, 1.103	1.115, 1.104	1.118, 1.104	1.122, 1.105	1.127, 1.105	1.134, 1.106	1.111, 1.104
	d_2	2.054	2.036	2.022	2.040	2.009	2.005	2.020
	d_3	1.533	1.529	1.523	1.523	1.519	1.517	1.527
	θ_1	99.46	101.78	102.02	103.45	103.46	104.40	98.32
	θ_2	111.55	116.05	116.57	116.68	117.42	117.57	115.73
	θ_3	115.84	121.67	125.43	127.04	128.98	130.53	124.01
	θ_4	113.78	114.83	114.84	115.29	115.34	115.71	114.45
	θ_5	105.76	105.93	106.61	107.14	107.41	108.05	109.85
^a	θ_6	103.82	105.95	107.35	108.40	109.11	110.33	106.29
	q_{Mn}	0.215	0.210	0.204	0.193	0.192	0.185	0.219
	$q_{\text{ortho-C}}$	-0.079	-0.075	-0.072	-0.069	-0.065	-0.061	-0.088
	q_{H}	0.038, 0.043	0.041, 0.045	0.041, 0.046	0.041, 0.048	0.041, 0.048	0.039, 0.050	0.040, 0.048

^a The definitions of the structural parameters are defined in Figure S2

Tables S5. The bond angle sum around the active *ortho*-C site of MCNTs (M = Mn and Co) (in degree).

n	MnCNT(n,n)	CoCNT(n,n)
3	329.81	316.21
4	344.30	—
5	349.07	343.69
6	350.39	—
7	352.94	348.68
9	354.44	351.50

Bond angle sum is defined in Figure 4a.

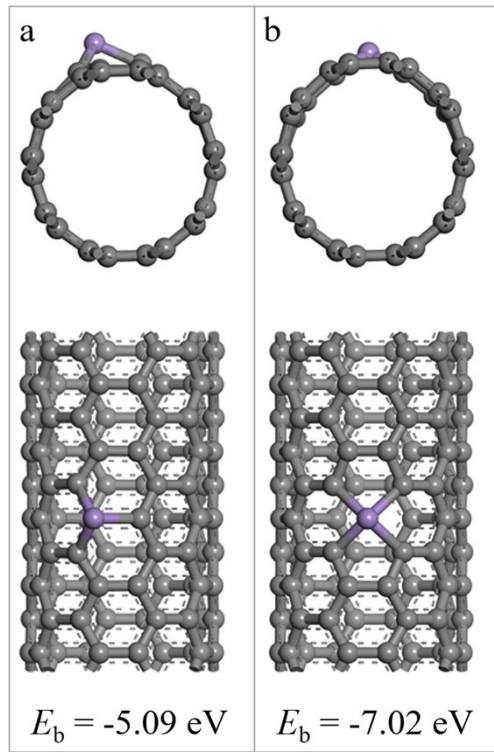


Figure S1. The monatomic substitution at a (a) monovacancy and (b) divacancy of CNT(5,5). The corresponding binding energies E_b of the Mn atom are given in eV. The purple and gray balls represent manganese and carbon atoms, respectively.

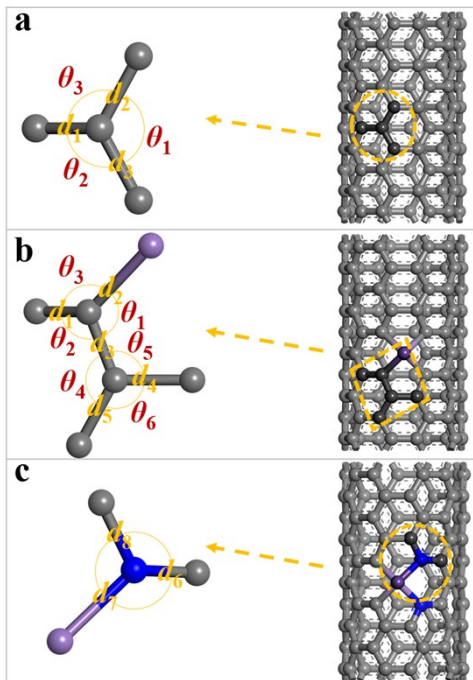


Figure S2. Representative configurations and definition of important structural parameters for the studied CNT(n,n) and MnCNT(n,n) ($n = 3, 4, 5, 6, 7$, and 9) and MnN₂CNT(5,5). (a) CNT(5,5), (b) MnCNT(5,5), and (c) MnN₂CNT(5,5). The purple and blue balls represent manganese and nitrogen atoms, respectively, while the gray and black balls represent carbon atoms.

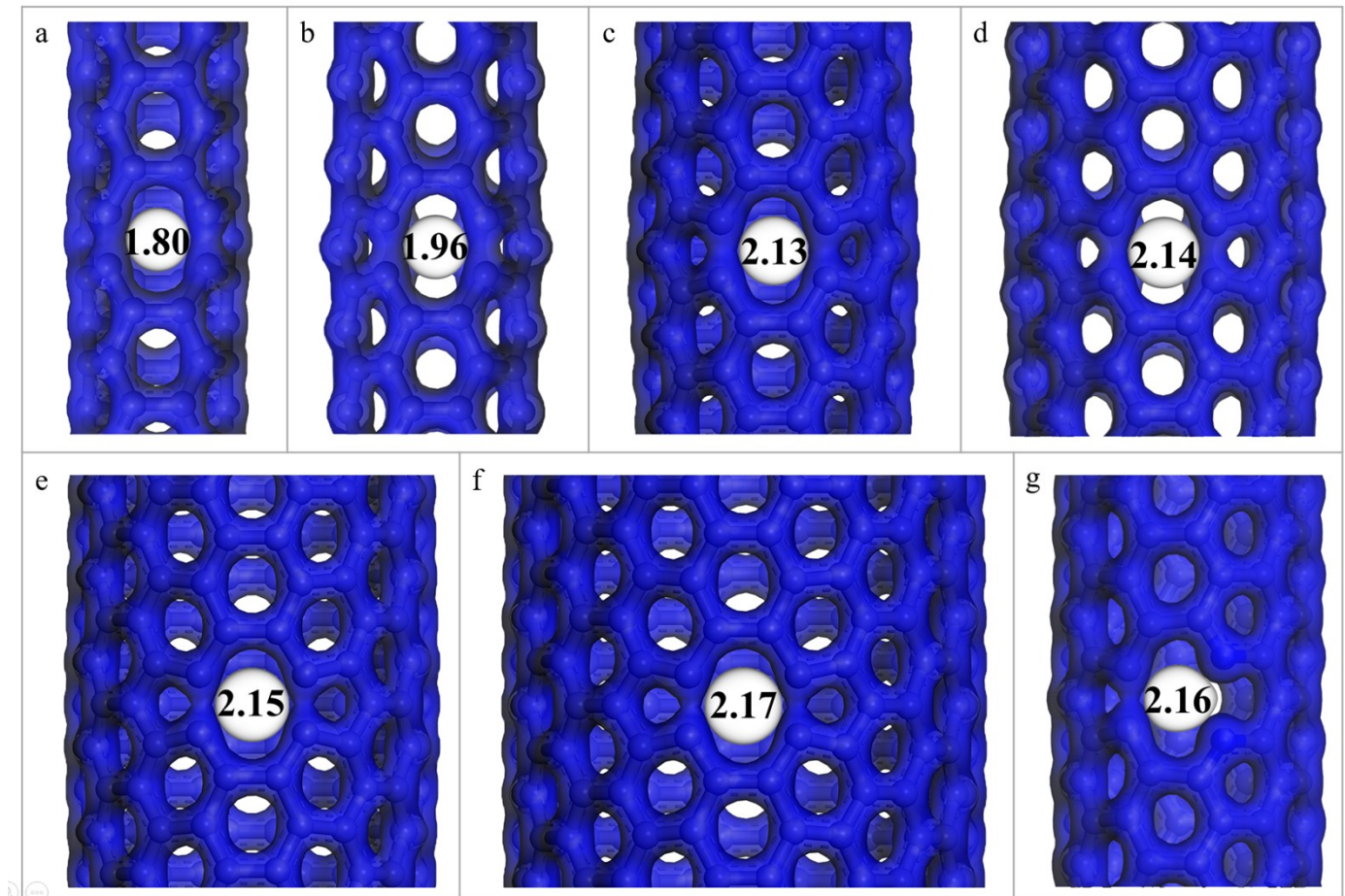


Figure S3. Electron density isosurfaces of di-vacant (a) CNT(3,3), (b) CNT(4,4), (c) CNT(5,5), (d) CNT(6,6), (e) CNT(7,7), (f) MnCNT(9,9) and (g) N₂CNT(5,5). The inscribed circles correspond to the electron deficiency center. The iso-value is 0.7 e/Å³, and numbers are the diameters of the circles in Å.

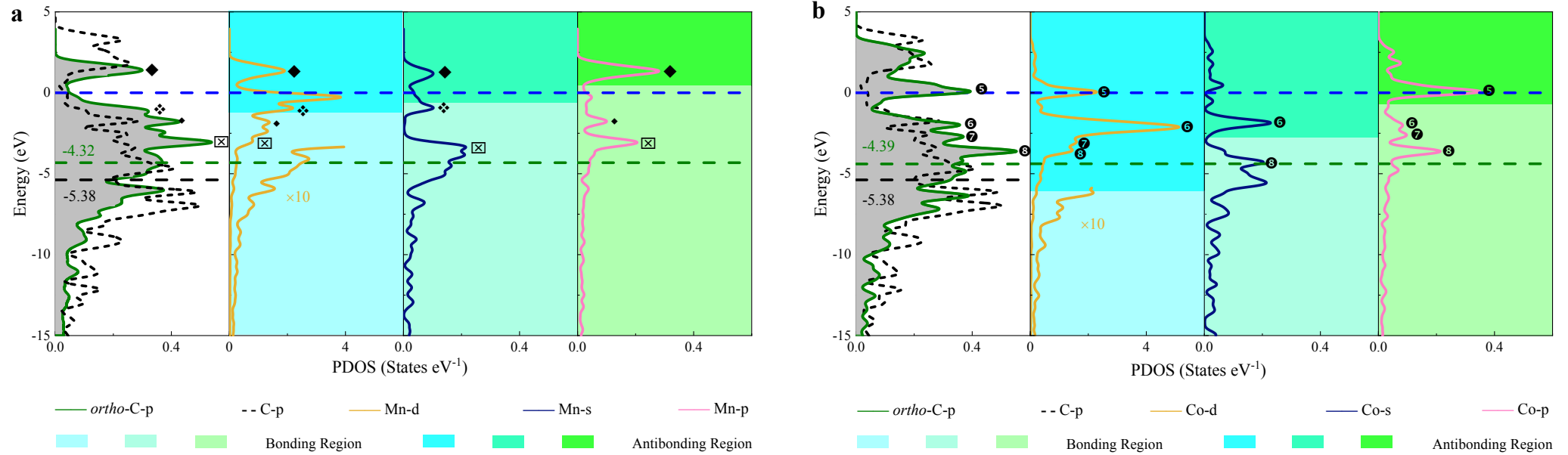


Figure S4. The detailed analysis of the upshift of p band center (ε_p) of the active C atom caused by metal doping. (a) MnCNT(5,5) and (b) CoCNT(5,5). For comparison, the projected density of states (PDOSs) of the C p band of the corresponding CNT(5,5) are also shown (black dot lines), and the band centers (in eV) are marked by black dashed lines.

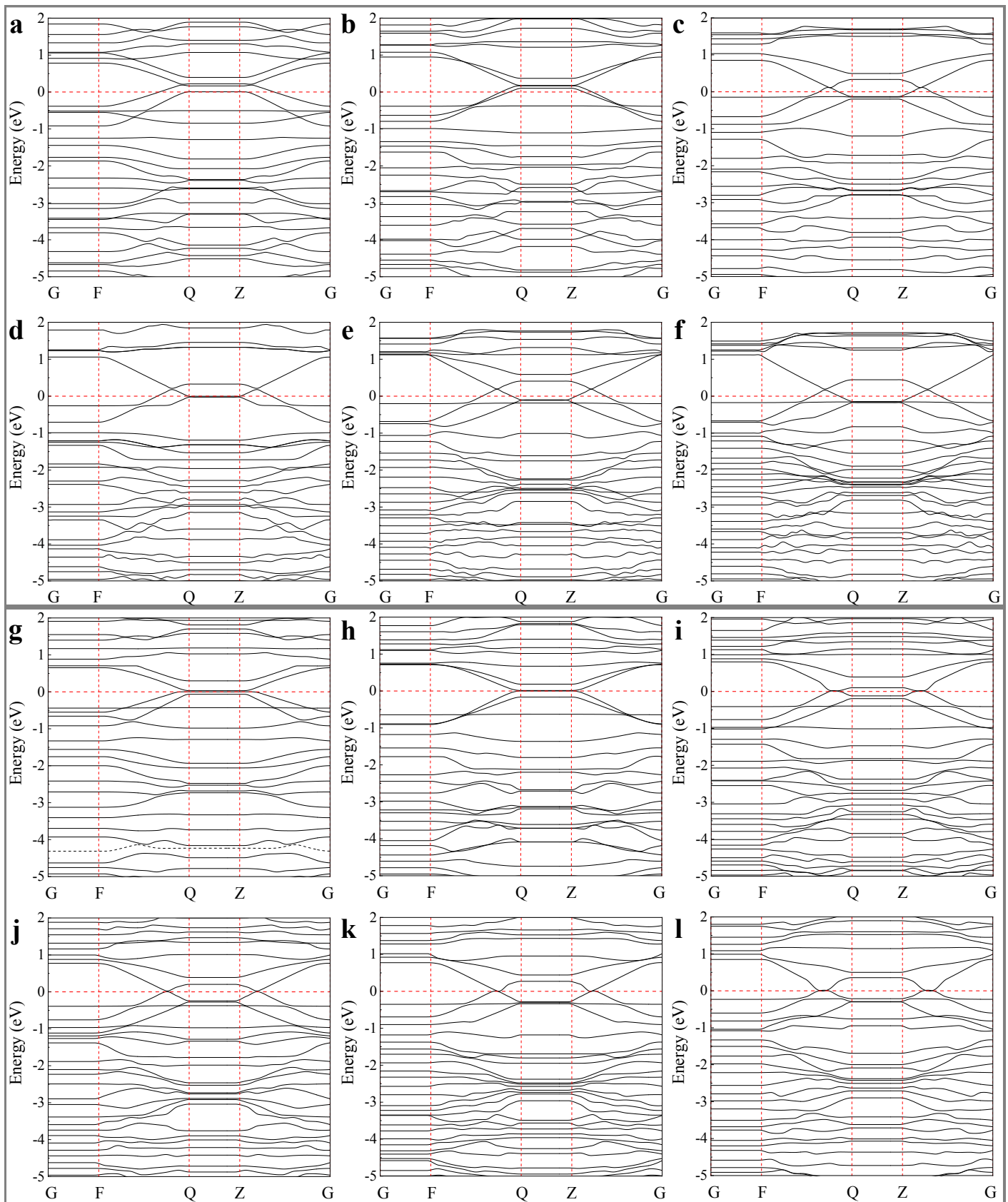


Figure S5. Energy band structures of (a,g) MnCNT(3,3), (b,h) MnCNT(4,4), (c,i) MnCNT(5,5), (d,j) MnCNT(6,6), (e,k) MnCNT(7,7) and (f,l) MnNCT(9,9) calculated by (a-f) PBE-D2 method and (g-l) PBE0 XC hybrid functional including ab-initio van der Waals correction. The Fermi level represented by red dash line is set as zero.

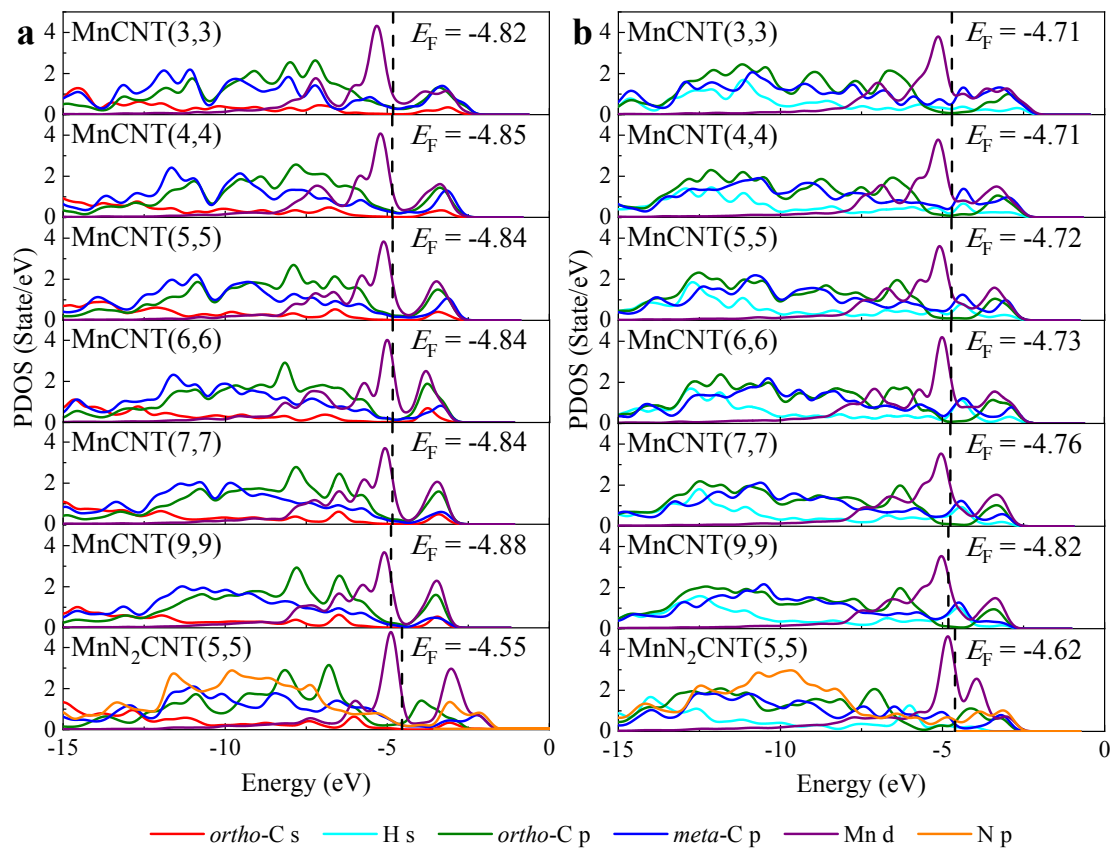


Figure S6. Projected density of states (PDOS) of (a) pristine and (b) first hydrogen adsorbed MnCNTs and MnN₂CNT(5,5). The vacuum level is set as zero. The PDOS intensity of C/H-s and C-p states is magnified ten-fold and five-fold, respectively.

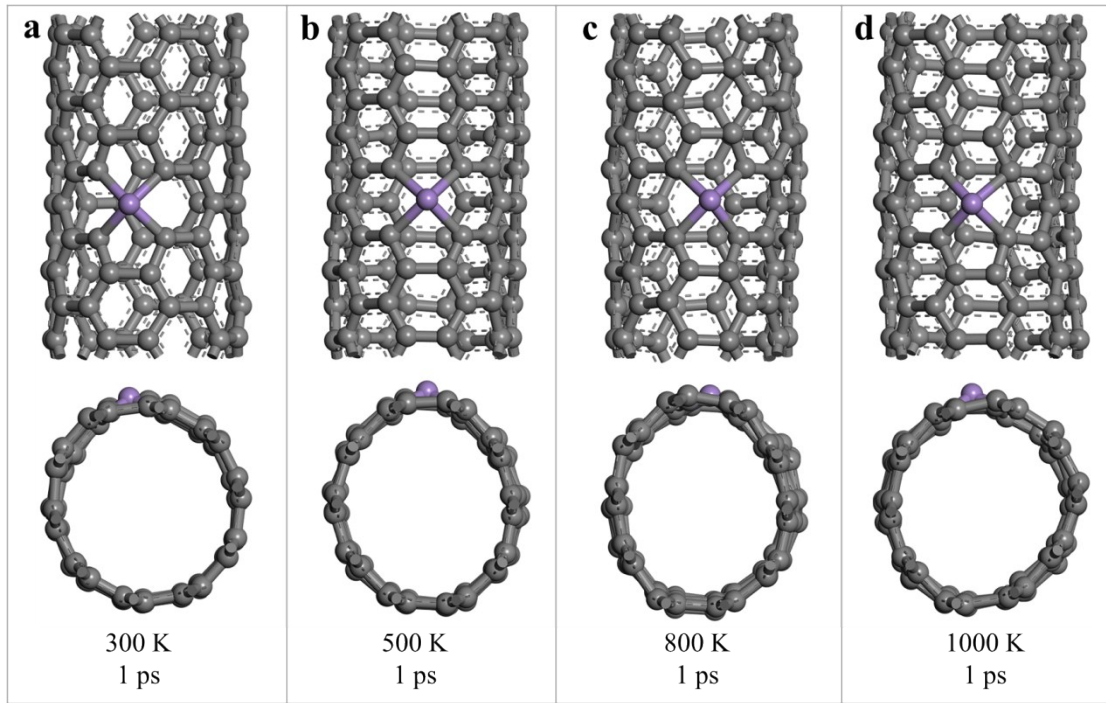


Figure S7. The final structures of MnCNT(5,5) after 1 ps first-principle molecular dynamics simulations at (a) 300 K, (b) 500 K, (c) 800 K, and (d) 1000 K. The purple and gray balls represent manganese and carbon atoms, respectively.

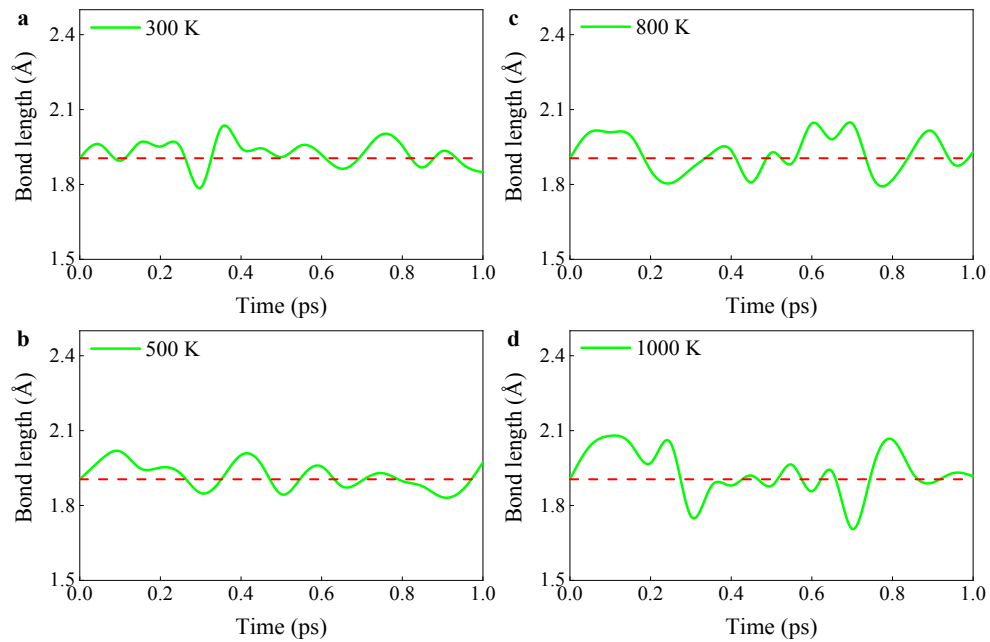


Figure S8. The change of Mn–C bond length in MnCNT(5,5) in first-principle molecular dynamics simulation at (a) 300 K, (b) 500 K, (c) 800 K and (d) 1000 K. The red dash line refers to the Mn–C bond length in the optimal structure. The values are recorded every 50 fs.

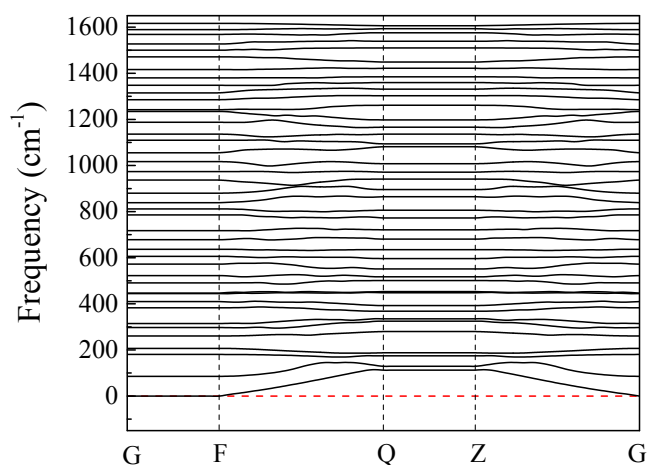


Figure S9. Phonon dispersion spectrum of the MnCNT(5,5) structure. Red dash line corresponds to the zero frequency.

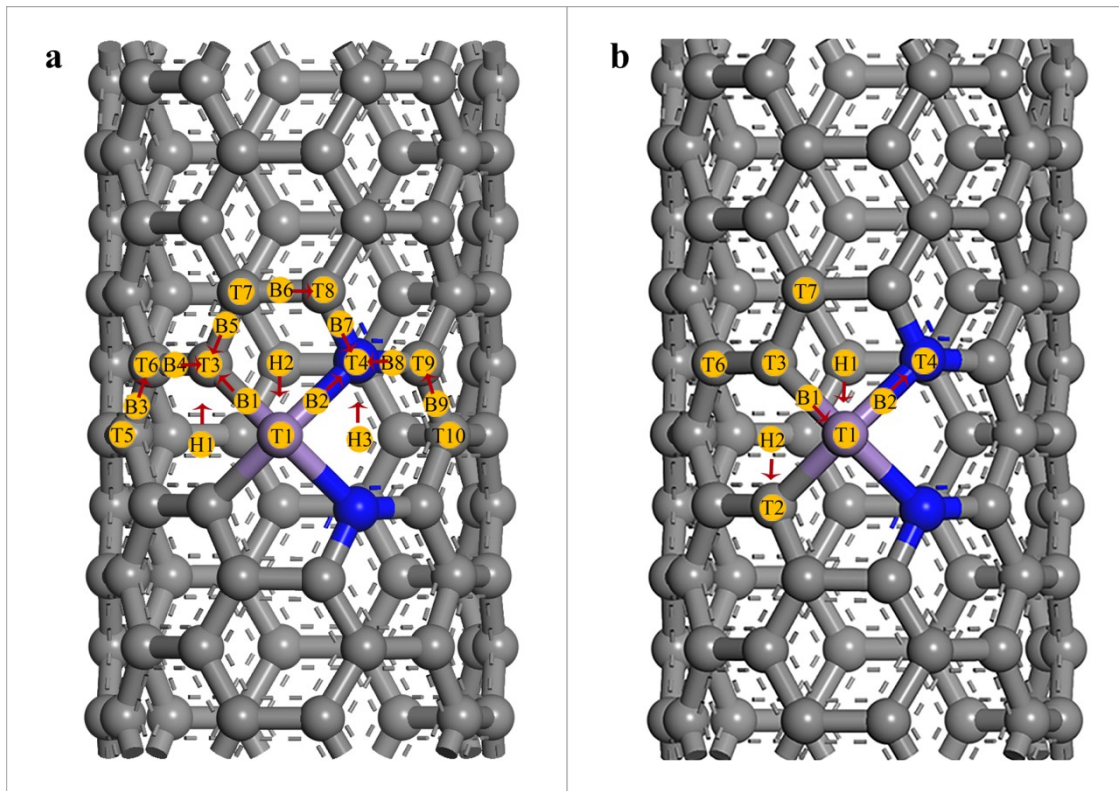


Figure S10. All possible adsorption sites for (a) first hydrogen atom and (b) second hydrogen atoms on MnCNT(n,n)s ($n = 3, 4, 5, 6, 7$, and 9) and MnN₂CNT(5,5). The T3 site is occupied by first hydrogen atom during considering the adsorption sites for second hydrogen atoms. The top, bridge, and hollow sites are represented by Tn, Bn, and Hn, respectively. The red arrows indicate the hydrogen atomic transfer during geometric optimization. The gray, blue, and purple balls represent carbon, nitrogen, and manganese atoms, respectively.

Adsorption sites of first/second H on MnCNT(n,n)s and MnN₂CNT(5,5)

For the adsorption of first H atom (FHA), 21 possible adsorption sites (Figure S8a) were explored, including 9 top sites (T1 (Mn), T2/T3 (*ortho*-C), T7/T8 (*meta*-C), T5, T6, T9 and T10 sites), 9 bridge sites (B1/B2, B3, B4, B5, B6, B7, B8 and B9 sites), and 3 hollow sites (H1, H2 and H3 sites). The calculated results suggest that only T1, T3, T4, T5, T6, T7, T8, T9, and T10 sites are feasible adsorption sites. The calculated adsorption energies (see Table S3) suggest the optimal first H adsorption site is T3 site (*ortho*-C) for all considered MnCNT(n,n) ($n = 3, 4, 5, 6, 7$, and 9) and MnN₂CNT(5,5), whose most stable configurations are shown in Figure S9. Especially, only the T3 site shows a negative H adsorption energy in MnCNT(n,n) ($n = 4, 5, 7$, and 9), while the others are positive.

Based on the first H atom adsorbed at the *ortho*-C site (T3 site in Figure S10b), the adsorption site of second H atom (SHA) is filtered by the calculations of adsorption

energies for all possible adsorption sites (Figure S10b). Among 9 possible sites (including 5 top sites, 2 bridge sites, and 2 hollow sites), only 5 possible sites serve as adsorption sites, due to the drift of second H atom during geometric optimization. The T7 site (*meta*-C) is the most likely to be an adsorb site for second H atom, due to its strongest adsorption energy (see Table S3).

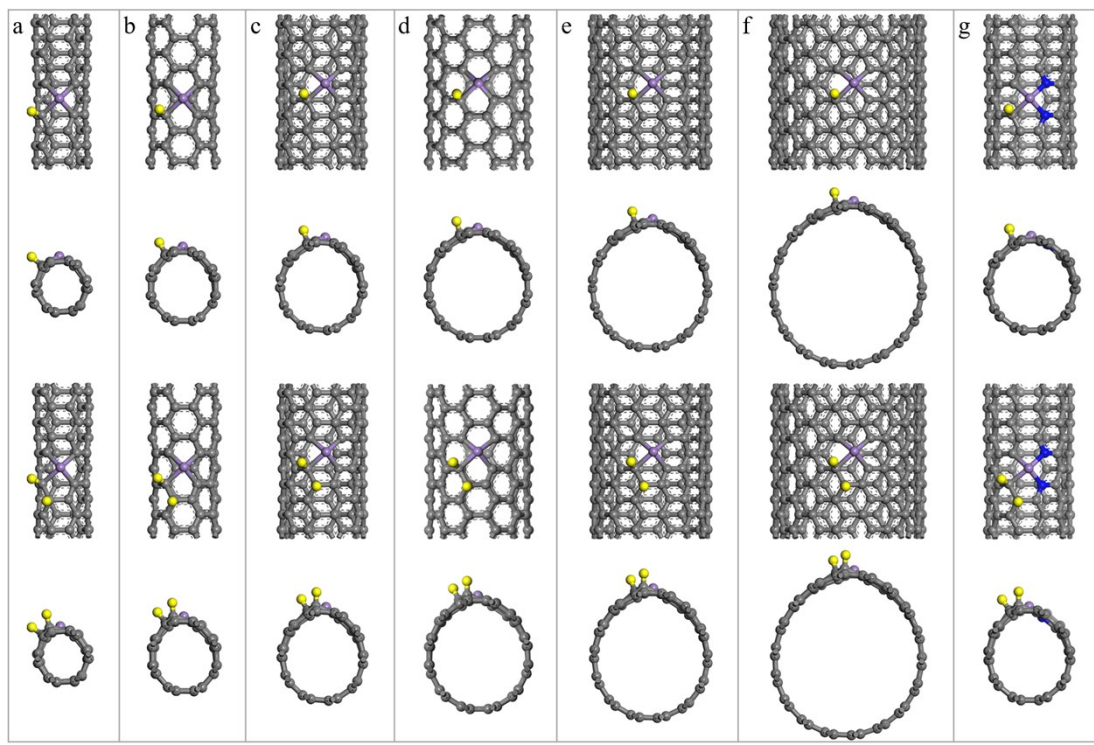


Figure S11. Top and side views of the most stable configurations of the first and second hydrogen adsorption on (a) MnCNT(3,3), (b) MnCNT(4,4), (c) MnCNT(5,5), (d) MnCNT(6,6) (e) MnCNT(7,7), (f) MnCNT(9,9) and (g) MnN₂CNT(5,5). The yellow, purple, blue, and gray balls represent the hydrogen, manganese, nitrogen, and carbon atoms, respectively

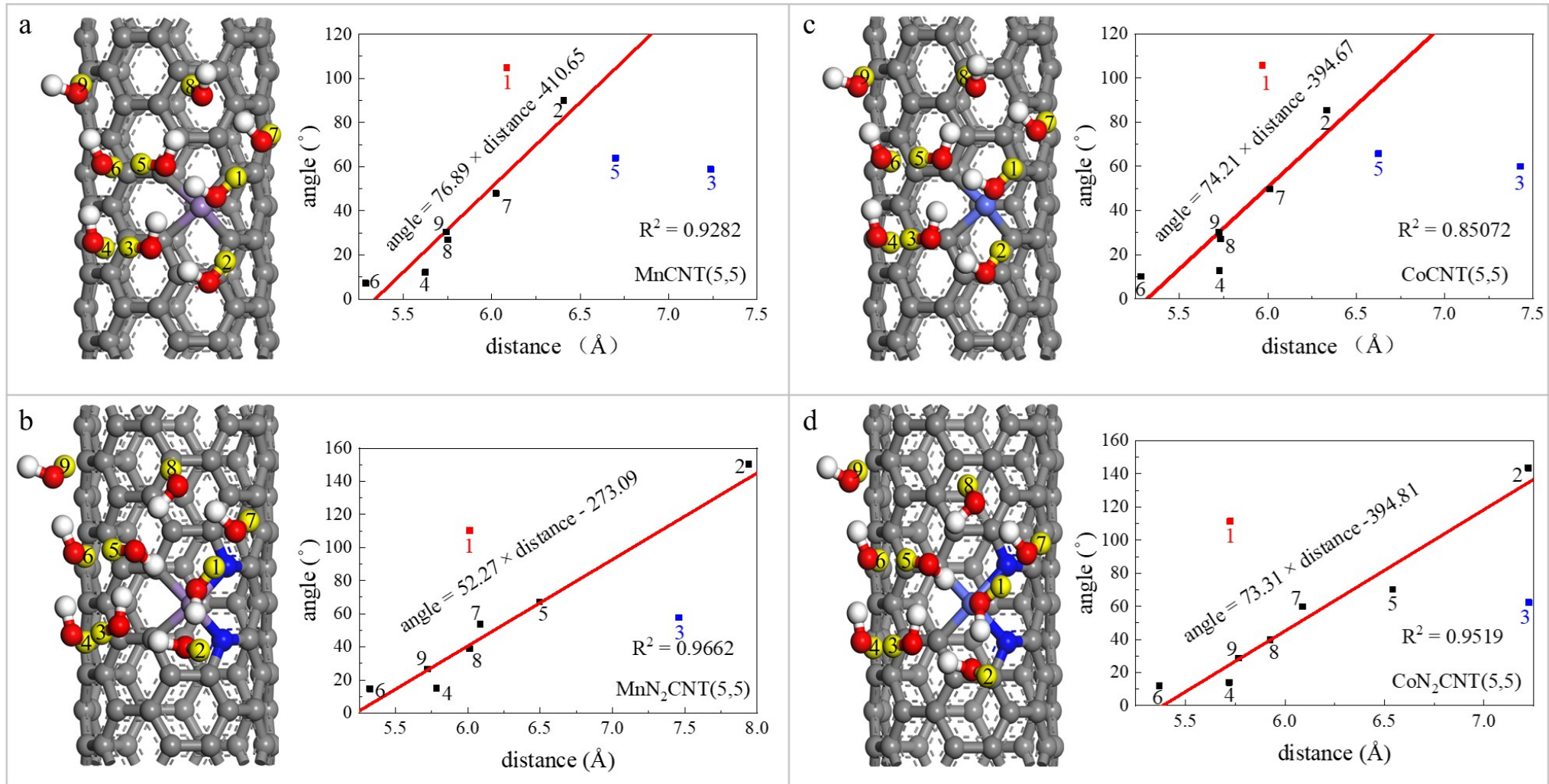


Figure S12. The radial distribution of hydrogen atoms for (a) MnCNT(5,5), (b) MnN₂CNT(5,5), (c) CoCNT(5,5) and (d) CoN₂CNT(5,5). The yellow balls with numbers represent the hydrogen atoms counted in the radial distribution. The white, gray, purple, blue, cyan balls represent hydrogen, carbon, manganese, nitrogen, cobalt atoms, respectively. The red trend lines are fitted by the black dots in the radial distribution.

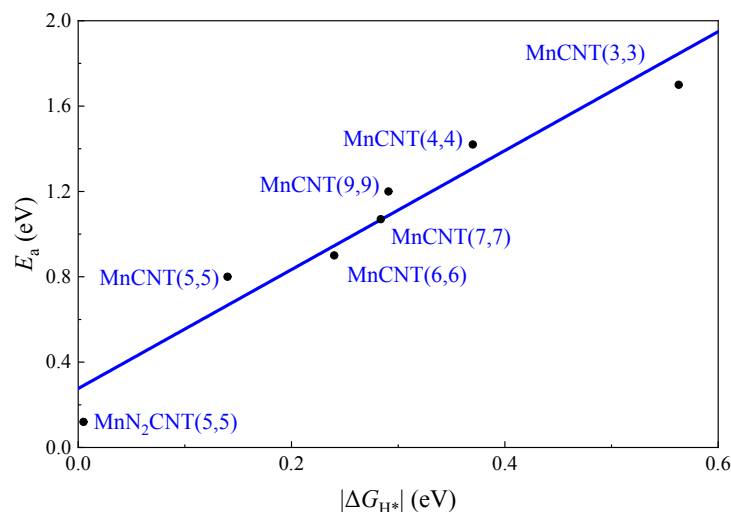


Figure S13. The relationship between activation barrier (E_a) of the rate-determining step (Heyrovsky reaction) and absolute hydrogen adsorption energy ($|\Delta G_{H^*}|$) on MnCNT(n,n)s and MnN₂CNT(5,5) at U = 0 V, pH = 0, and T = 298 K.

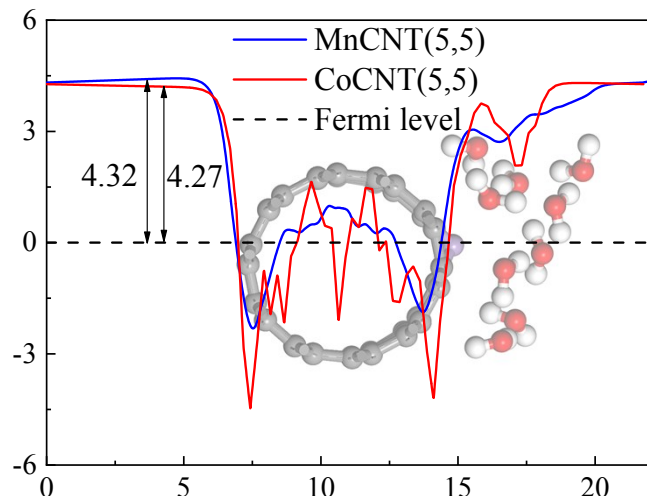


Figure S14. The electronic potential profiles averaged on the plane perpendicular to b -axis as a function of the b -axis of the supercell of MnCNT(5,5) and CoCNT(5,5), respectively. The structure of MCNT(5,5) ($M = \text{Mn}$ or Co) with water layer is shown in the background.

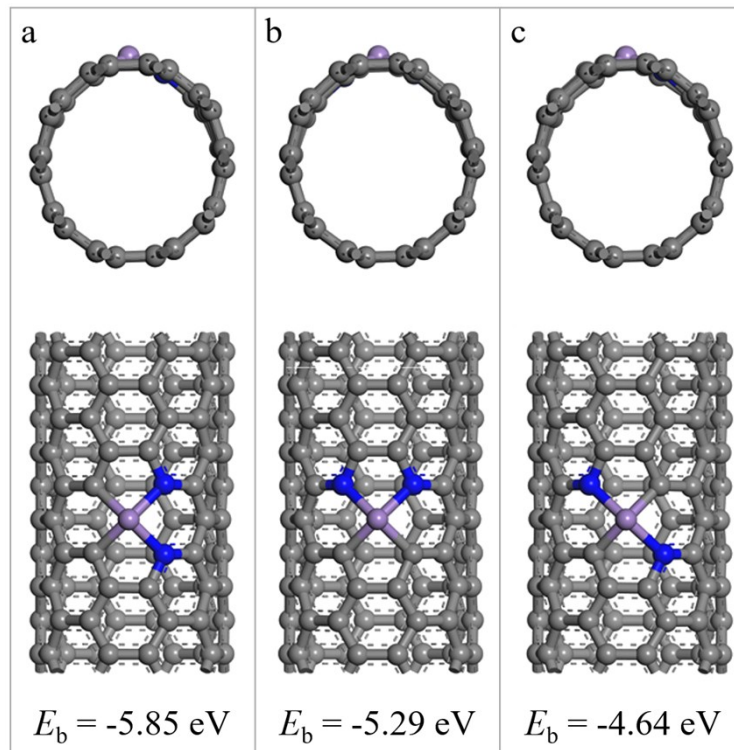


Figure S15. The possible configurations of $\text{MnN}_2\text{CNT}(5,5)$ with the two nitrogen atoms located (a) parallel to, (b) perpendicular to, and (c) oblique to the c axis of CNT. The corresponding binding energies E_b of the Mn atom are given in eV. The gray, blue and purple balls represent carbon, nitrogen, and manganese atoms, respectively.